AAPS PharmSciTech, Vol. 12, No. 3, September 2011 (© 2011)
DOI: 10.1208/s12249-011-9637-7

Research Article

Theme: Advances in Pharmaceutical Excipients Research and Use: Novel Materials, Functionalities and Testing
Guest Editors: Otilia Koo, Thomas Farrell, Allison Radwick, Sameer Late

Analysis of Structural Variability in Pharmaceutical Excipients Using Solid-State NMR Spectroscopy

Diana M. Sperger[1] and Eric Jon Munson[1,2,3]

Received 29 October 2010; accepted 23 May 2011; published online 28 June 2011

Abstract. Polysaccharide-based excipients comprise the majority of most solid dosage forms and can vary dramatically in terms of structural and functionally related properties. Analytical methods for characterizing these important formulation components are crucial. Solid-state NMR spectroscopy (SSNMR) can provide a wealth of information on these materials while offering the advantages of non-destructive sample preparation and selectivity. The overall objective of this work is to identify SSNMR parameters that can be used to detect differences among these excipients. Excipients were obtained from a wide range of suppliers and analyzed as received; ^{13}C SSNMR spectra were acquired using a Chemagnetics CMX-300 spectrometer operating at approximately 75 MHz. The resolution of SSNMR signals of many excipients allows for positive identification of the major form present. Alginic acid and sodium alginate can be differentiated based on carbonyl peak position. Analysis of relative peak intensities provides insight into the purity of a carrageenan sample compared to known standards. The SSNMR spectrum of starch can be used to identify the source and to quantitate the amorphous and crystalline content. Relaxation values and peak areas of starch derivatives can be related to the degree of hydrolysis, providing an alternative method for determining dextrose equivalent. Differences in peak intensities and relaxation time values of HPMC samples can be correlated to the amount of methoxy subsituent groups. Important characteristics of excipients such as form identification, structural differences, crystalline and amorphous content, and water content variations can be detected using SSNMR spectroscopy.

KEY WORDS: excipients; polysaccharide; relaxation time; solid-state NMR spectroscopy.

INTRODUCTION

The majority of pharmaceuticals are marketed in the solid state, with excipients constituting the largest component of most formulations. Many of these excipients are polysaccharides and are derived from natural products. Multiple companies manufacture these excipients on large scales, using various processes, in numerous locations, and at different times of the year. Thus, variability among naturally derived excipients from different suppliers is inevitable. Similarly, changes or updates to a company's manufacturing process or source of raw materials can result in lot-to-lot variability. This variability may significantly impact the physicochemical properties and hence functionality of the excipient in the final dosage form. Therefore, it is important to have analytical methods in place for accurately assessing and identifying differences in these materials (1).

Solid-state NMR (SSNMR) spectroscopy is a valuable tool for the structural analysis of polysaccharide-based excipients, as the amorphous or semi-crystalline nature of these materials limits the capability of more commonly used solid-state techniques such as differential scanning calorimetry and powder X-ray diffraction (PXRD) (2). A major advantage of SSNMR spectroscopy is that it is a non-destructive and selective technique that allows characterization of the excipient directly in the physical state in which it is to be administered, even when in the presence of other excipients and the active pharmaceutical ingredient (3). Additionally, SSNMR spectroscopy can provide unique insight into the molecular dynamics of pharmaceutical solids such as excipients through the use of relaxation measurements (4).

The overall objective of this work is to identify the SSNMR parameters that can be used to detect differences in structural properties among some common polysaccharide-based excipients. Excipient systems for analysis include alginic acid and alginate, carrageenans, starch and derivatives,

[1] Department of Pharmaceutical Chemistry, University of Kansas, Lawrence, Kansas, USA.
[2] Department of Pharmaceutical Sciences, University of Kentucky, 789 South Limestone Street, Lexington, Kentucky 40536, USA.
[3] To whom correspondence should be addressed. (e-mail: eric.munson@uky.edu)

and cellulose-based excipients such as microcrystalline cellulose, carboxymethylcellulose sodium, hydroxyethylcellulose (HEC), hydroxypropylcellulose (HPC), and hydroxypropylmethylcellulose (HPMC). Parameters assessed via SSNMR spectroscopy include chemical shift (peak position), relative signal areas and intensities, and proton relaxation times (^{1}H T_1 and ^{1}H $T_{1\rho}$).

MATERIALS AND METHODS

Samples

The excipients that were studied are listed in Table I. Cases in which different forms, grades/types, or lots of an excipient were analyzed are also specified in Table I. All excipients were stored at ambient temperatures with desiccant and analyzed as received without further modification.

Water Content

Thermogravimetric analysis (TGA) using a TA Q50 Thermogravimetric Analyzer (TA Instruments, New Castle, DE) was used to determine the water content of some of the as-received excipients. Approximately 10–15 mg of each sample was heated to 105°C at a heating rate of 20°C/min and held isothermally for 180 min. Total weight loss was attributed to water content of the sample.

Solid-State NMR Spectroscopy

Solid-state ^{13}C NMR spectra were acquired using a Chemagnetics CMX-300 spectrometer (Varian, Inc., Palo Alto, CA) operating at approximately 75 MHz for ^{13}C. Chemagnetics double-resonance probes equipped with either PENCIL™ 7.5-mm spinning modules or Revolution NMR 7-mm spinning modules (Revolution NMR, LLC, Fort Collins, CO) were used to acquire all spectra. Samples were packed into zirconia rotors and sealed with either Kel-F or Teflon end caps. Spectra were acquired using variable-amplitude or ramped-amplitude cross-polarization (6) magic-angle spinning (7) at 4.0 kHz, contact times of 1 to 2 ms, and high-power ^{1}H-decoupling fields of approximately 60–70 kHz. Total sideband suppression (8) and SPINAL64 decoupling (9) were used when possible. 3-Methylglutaric acid was used to optimize the spectrometer settings and set the reference frequency (10). The recycle delays varied based upon ^{1}H T_1 values for each excipient, which were measured using saturation recovery experiments. Using KaliedaGraph (Synergy, version 4.01), plots of integrated signal areas

Table I. Excipient Samples Used in this Study

Excipient	Supplier (Grade)	Number of lots	Functional category (5)
Alginic acid	FMC Biopolymer (120 NM)	1	Stabilizing agent; suspending agent; tablet binder; disintegrant; viscosity-increasing agent
	Sigma	1	
	Spectrum	1	
Sodium alginate	FMC Biopolymer (LF 10/60LS)	1	
	Aldrich	1	
	Spectrum	1	
ι-Carrageenan	FMC Biopolymer	2	Emulsifying agent; stabilizing agent; sustained release matrix; viscosity-increasing agent
	Sigma	2	
	Fluka	1	
κ-Carrageenan	FMC Biopolymer	2	
	Fluka	1	
λ-Carrageenan	FMC Biopolymer	2	
	Fluka	1	
Carrageenan	Sigma	1	
	Spectrum	2	
Starch (corn)	Grain Processing (B880, B700)	1 of each	Glidant; tablet diluent and binder; disintegrant
	Sigma	1	
Starch (potato)	Sigma	1	
Starch (wheat) potato	Sigma	1	
Maltodextrin	Aldrich (419672, 419680, 419699)	1 of each	Coating agent; tablet diluent and binder
Corn syrup solids	Grain Processing (M200, M250)	1 of each	
	Globe (42DE)	1	
Avicel avicel	FMC Biopolymer (PH101, PH102)	2 of each	Tablet diluent/binder
	FMC Biopolymer (PH105, PH112, PH113)	1 of each	
HEC	Spectrum	2	Coating agent; sustained release agent; tablet binder; viscosity-increasing agent
	Aldrich	1	
HPC	Spectrum	3	
	Aldrich	1	
HPMC	Spectrum (type 2208)	2	
	Spectrum (type 2910)	1	
	Sigma (type 2910)	1	
Carboxymethyl-cellulose sodium	Fluka	1	Tablet binder/disintegrant; viscosity increasing agent
	Acros Organics	3	

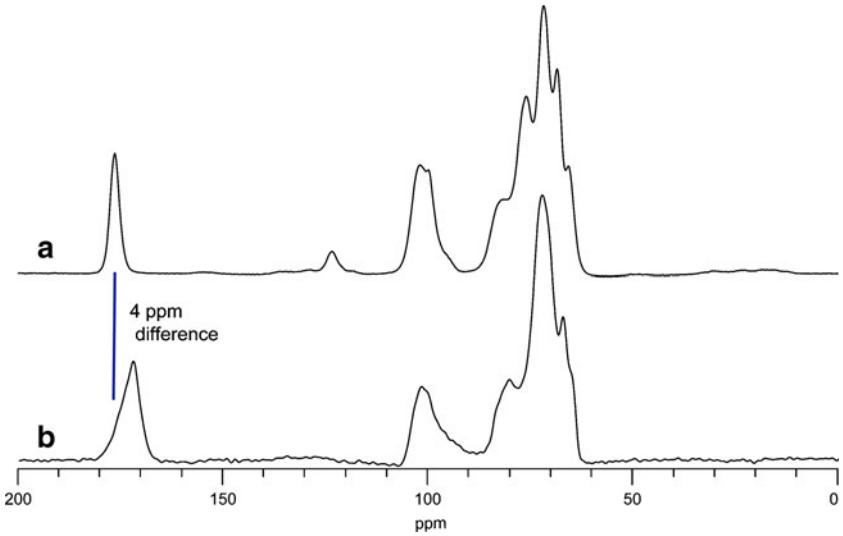

Fig. 1. Representative ^{13}C SSNMR spectra of **a** sodium alginate and **b** alginic acid

versus saturation recovery times were fit to the equation $y = \text{amp}\left(1 - e^{-\tau/T_1}\right)$ where y is the integrated signal area, amp is the amplitude constant, τ is the saturation recovery time, and T_1 is the spin–lattice relaxation time. A recycle delay equal to at least 1.5 times the ^1H T_1 value of each sample was used to acquire each spectrum. To determine ^1H $T_{1\rho}$ values, multiple-contact time experiments were performed and the rate of magnetization decay was calculated using Chemagnetics Spinsight software. When necessary, deconvolution of signals to aid in calculation of peak areas and intensities was achieved using Chemagnetics Spinsight software.

RESULTS AND DISCUSSION

Alginic Acid and Sodium Alginate

Alginic acid and sodium alginate are linear unbranched polysaccharides extracted from certain seaweed species. Both contain various proportions of β-D-mannuronic acid (M) and α-L-guluronic acid (G) residues, with the only chemical difference between them being the protonation or deprotonation of the carboxylic acid group (11). Representative ^{13}C SSNMR spectra of alginic acid and sodium alginate are shown in Fig. 1. While there are some differences in relative peak intensities in the region 60–110 ppm, too much overlap exists in this part of the spectrum to be able to use it to distinguish between the two forms. However, the chemical shift of the peak to the far left in each spectrum, corresponding to the carbonyl carbon, is significantly different depending on which alginate form (acid or sodium salt) is present. As shown in Table II, the carbonyl peak position consistently occurs at ~172 ppm in all alginic acid samples and at ~176 ppm in all sodium alginate samples. Thus, although alginic acid and sodium alginate are very structurally similar, they can be identified and distinguished based on the carbonyl peak position in the SSNMR spectra. While this can be achieved using other techniques, SSNMR spectroscopy offers the advantage of non-destructive sample preparation and selectivity that enables form identification in the presence of other materials.

The differences in relative peak intensities in the region 60–90 ppm noted in Fig. 1 are further illustrated in Fig. 2; the ^{13}C SSNMR spectra of three sodium alginate samples obtained from different suppliers is shown. While these differences are not useful for distinguishing between the acid and sodium salt forms of alginate, variations in this region do reflect differences in monomer composition. As shown in Fig. 2, signals in this area of the spectrum can be assigned as either G or M residues, based on solution-state NMR values (12) and a previous study of sodium alginate by SSNMR spectroscopy (13). Upon examination of Fig. 2, it can be clearly seen that the sample from FMC Biopolymer contains more G monomer than those from Spectrum and Aldrich, as the signals corresponding to the G monomer are dominant in the FMC Biopolymer

Table II. Differences in Carbonyl Chemical Shift Value for Alginic Acid and Sodium Alginate

Carbonyl chemical shift values			
Alginic acid		Sodium alginate	
Supplier	Peak position (ppm)	Supplier	Peak position (ppm)
FMC Biopolymer	172.1	FMC Biopolymer	176.5
Sigma	172.3	Aldrich	176.4
Spectrum	171.9	Spectrum	176.7

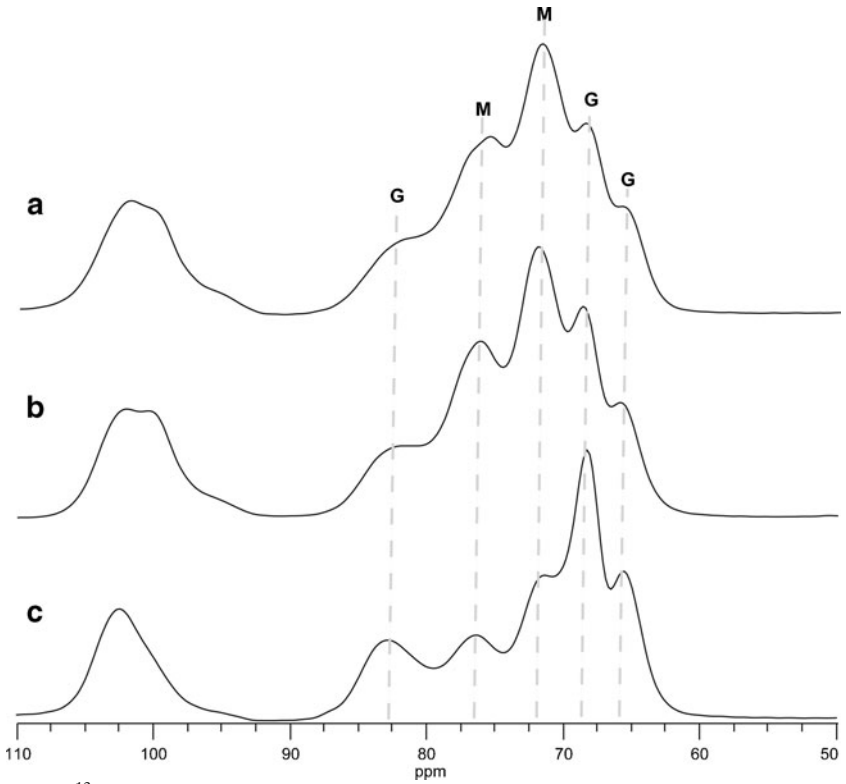

Fig. 2. ^{13}C SSNMR spectra of sodium alginate samples from **a** Aldrich, **b** Spectrum, and **c** FMC Biopolymer. Peaks labeled *G* and *M* correspond to ring carbons of the guluronic and mannuronic acid residues, respectively

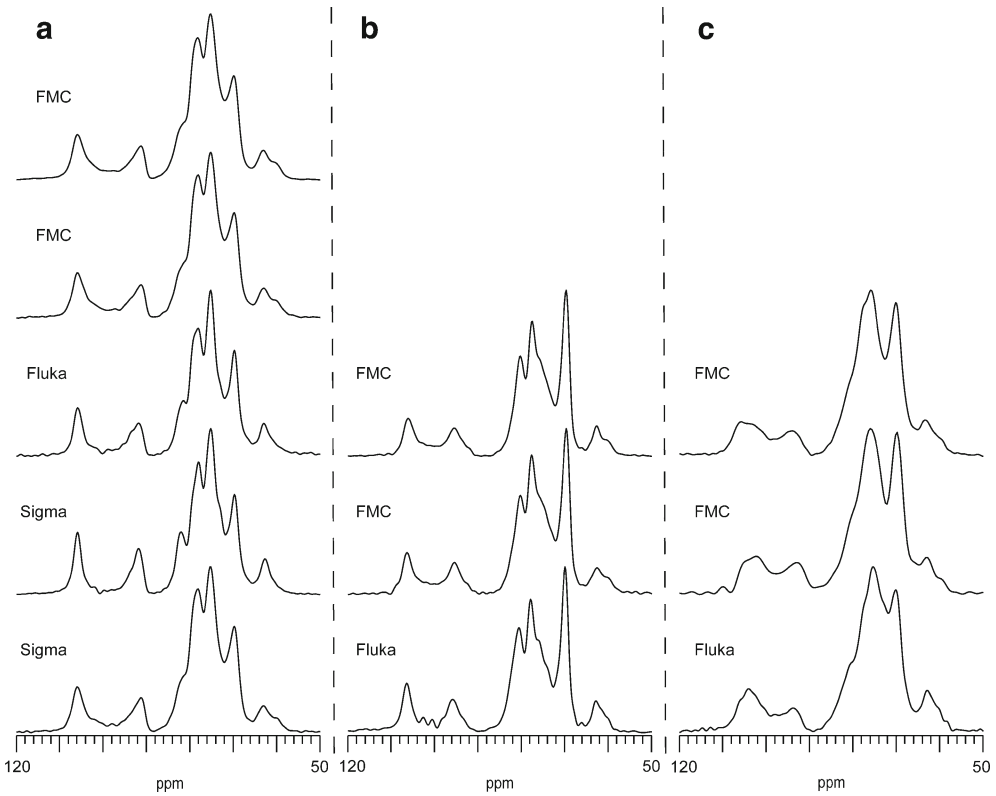

Fig. 3. ^{13}C SSNMR spectra of carrageenan samples: **a** ι-forms, **b** κ-forms, and **c** λ-forms

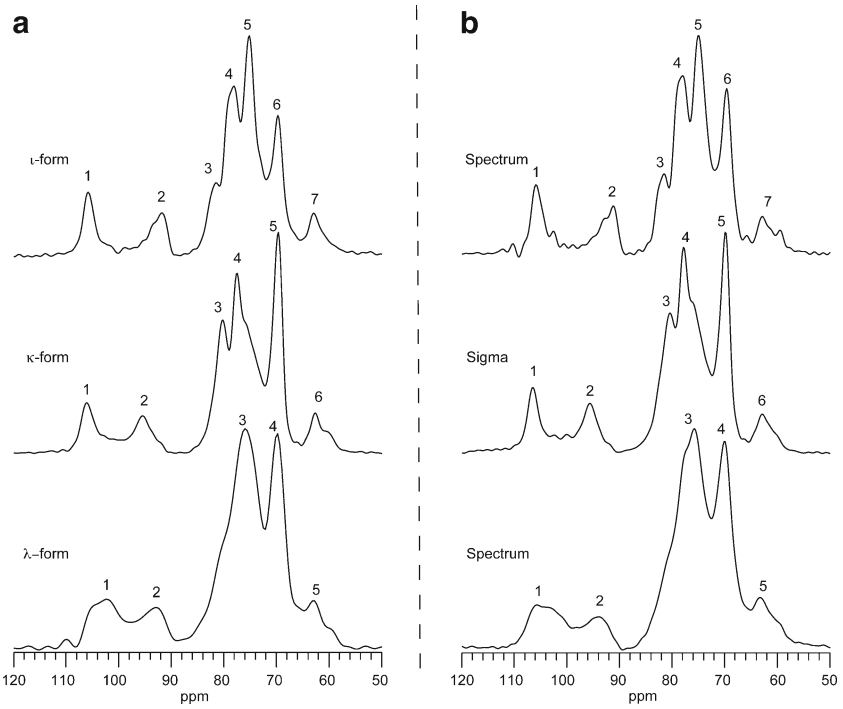

Fig. 4. ^{13}C SSNMR spectra of carrageenan samples: **a** "known" forms and **b** "unknown" forms

spectrum and less intense in the spectra of the other two samples. The relative intensities between G and M peaks in the SSNMR spectra of the sodium alginate samples from Spectrum and Aldrich are very similar, suggesting that these two materials contain comparable amounts of each monomer. Although outside the scope of this paper, quantitation of the G and M residues by SSNMR spectroscopy with the aid of spectral deconvolution is possible and has been demonstrated in a few cases (13,14). However, for various reasons, the values obtained do not always agree with those obtained via solution-state NMR analysis. Work performed in our laboratory to address this issue will be presented in a future manuscript.

Carrageenans

Like alginates, carrageenans are found in the cell walls of some species of seaweed. Carrageenan is primarily composed of a polysaccharide chain of alternating 1,3-linked β-D- and 1,4-linked α-D-galactopyranose residues, with sulfate groups located in various positions (15). The iota (ι), kappa (κ), and lambda (λ) forms of carrageenan are structurally different due to the varied presence and number of 3,6-anhydro-bridge and sulfate groups, which results in vast differences in gelling properties among the three forms. As shown in Table I, carrageenans are available as pure forms identified by the supplier, which

Table III. Summary of Differences in Relative Peak Intensities for "Known" and "Unknown" Carrageenan Samples

Peak	Chemical shift (ppm)	Relative intensity (normalized)	Peak	Chemical shift (ppm)	Relative intensity (normalized)	Peak	Chemical shift (ppm)	Relative intensity (normalized)
Knowns								
ι-form			κ-form			λ-form		
1	105.8–106	0.27–0.38	1	106.1–106.5	0.19–0.29	1	102.5–104.8	0.18–0.25
2	91.2–91.9	0.20–0.28	2	95.3–95.8	0.16–0.21	2	93.0–93.9	0.13–0.19
3	81.3–82.2	0.34–0.38	3	80.4	0.62–0.66	3	75.4–76.1	1.00
4	78.1–78.2	0.78–0.88	4	77.7–77.8	0.85–0.94	4	70.0–70.1	0.84–0.97
5	75.2–75.4	1.00	5	69.8–69.9	1.00	5	62.8–63.3	0.21–0.23
6	69.7–69.8	0.61–0.64	6	62.7–62.9	0.15–0.16	–	–	–
7	62.8–63.1	0.16–0.22	–	–	–	–	–	–
Unknowns/Mixtures								
Spectrum (lot 1)			Sigma			Spectrum (lot 2)		
1	105.4	0.27	1	106.5	0.30	1	103.6	0.18
2	91.5	0.23	2	95.7	0.22	2	93.9	0.14
3	82	0.36	3	80.4	0.66	3	75.8	1.00
4	78.4	0.86	4	77.8	0.95	4	70.0	0.93
5	74.8	1.00	5	69.8	1.00	5	63.3	0.21
6	69.8	0.73	6	62.6	0.15	–	–	–
7	62.6	0.19	–	–	–	–	–	–

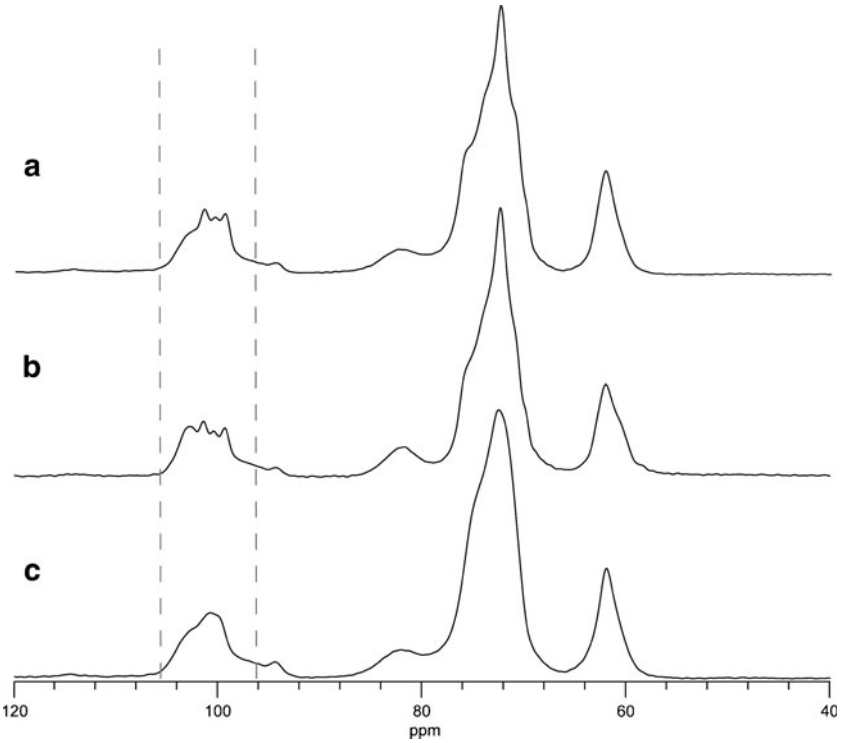

Fig. 5. Representative ^{13}C SSNMR spectra of **a** cornstarch, **b** wheat starch, and **c** potato starch. Differences in the C-1 region of the spectrum are highlighted

will be referred to as "known" samples, and also as forms or mixtures of forms not completely identified by the supplier, which will be referred to as "unknown" samples throughout the remainder of this manuscript.

The ^{13}C SSNMR spectra of the "known" samples identified as ι, κ, and λ are shown in Fig. 3a, b, and c, respectively. The first thing to note is the number of signals present in the SSNMR spectrum of each form. Discounting

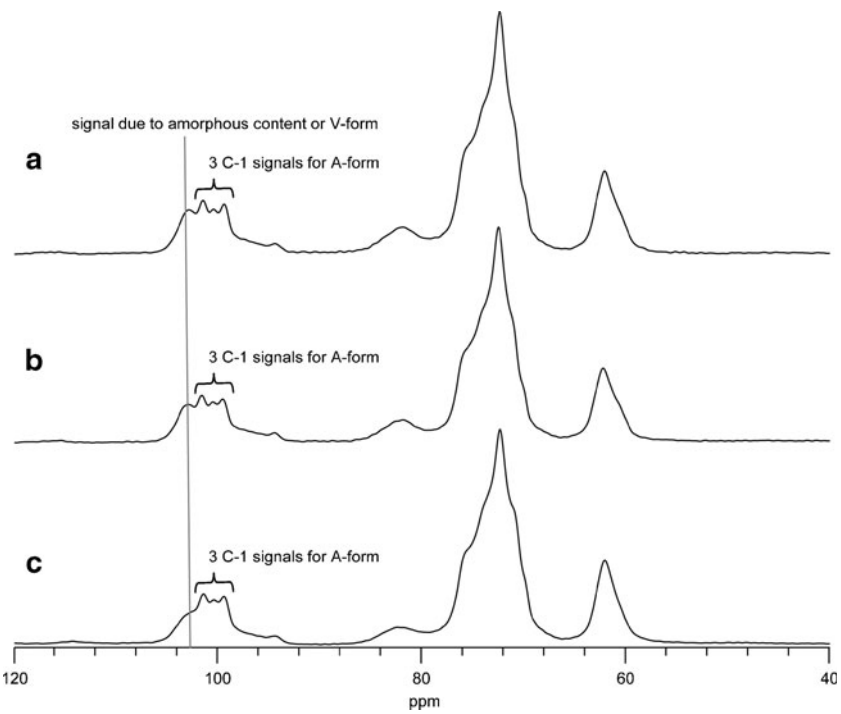

Fig. 6. ^{13}C SSNMR spectra of cornstarch: **a** Grain Processing B880, **b** Grain Processing B700, and **c** Sigma. Variations in crystalline versus amorphous and/or amylose content are highlighted

the slight shoulders that appear on some peaks, the spectra of all the ι-samples are resolved into seven distinct signals, those of the κ-samples into six distinct signals, and those of the λ-samples into just five signals. These data agree with a previous study (16), although we believe that this is the first report of seven distinct signals being observed for the ι-form. The earlier study compared only one sample each of ι- and κ-carrageenan and reported six chemical shifts for both forms (16). Advancements in SSNMR decoupling methods since the previous study are the likely reasons for this improved ability to resolve a seventh signal in the ι-form.

As shown in Fig. 3, the number of resolved peaks is consistent across all samples, regardless of supplier. However, slight differences between the spectra of samples from different suppliers can be observed. For instance, in the ι-forms (Fig. 3a), the SSNMR spectra of the two samples received from FMC Biopolymer are essentially identical. The SSNMR spectrum of one of the Sigma samples strongly resembles that of the FMC Biopolymer samples, but the spectra of the other Sigma sample and of the Fluka sample show sharper resolution between peaks and lack of the shoulder on the peak at ~60 ppm. It is likely that these two samples were obtained from different materials and/or by a different process. Differences between the FMC Biopolymer samples and Fluka sample of the λ-form are also observed (Fig. 3c). The SSNMR spectra of the κ-samples (Fig. 3b) are very similar, suggesting that the processes used to produce the κ-sample from Fluka and the κ-samples from FMC Biopolymer resulted in the same product and/or samples that produce the same SSNMR spectrum.

To better highlight the spectral differences between the three forms, an overlay of representative ^{13}C SSNMR spectra of the ι, κ, and λ-samples is shown in Fig. 4a. While there are differences in the peak shapes and positions of signals 1 and 2, the major distinction between forms occurs in the region 60–90 ppm. The changes in the number of peaks and relative intensities observed in this region are due to differences in the degree of sulfation between the three forms (16). In Fig. 4b, the ^{13}C SSNMR spectra of the "unknown" samples (Table I) are shown. It is clear upon visual examination that the spectra of the two Spectrum samples are dissimilar. The SSNMR spectrum of one lot is similar to that of the "known" ι-form while the SSNMR spectrum of the other lot matches that of the "known" λ-form. The Sigma sample appears to consist primarily of κ-carrageenan.

Table III outlines the range of chemical shifts and normalized relative intensity values for all of the "known" and "unknown" samples. The Sigma "unknown" sample has chemical shifts and normalized relative intensities that fall within the range of all "known" κ-forms that were analyzed.

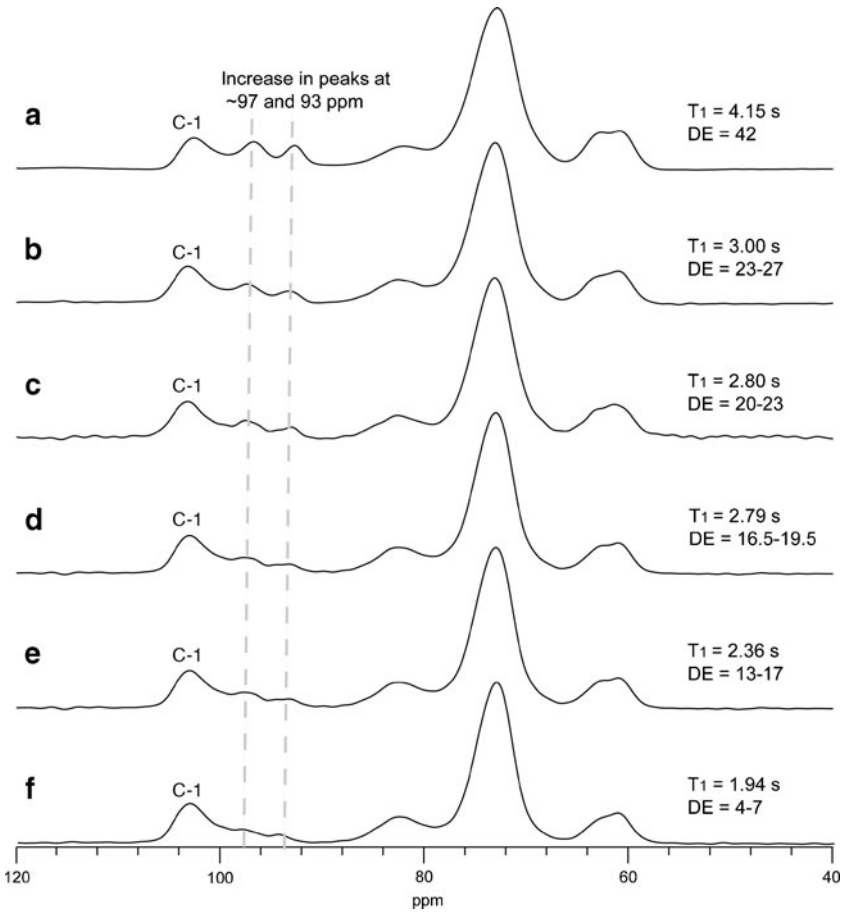

Fig. 7. ^{13}C SSNMR spectra of corn syrup solids: **a** Globe, **b** Grain Processing M250, **c** Grain Processing M200, and maltodextrins: **d** Aldrich 419699, and **f** Aldrich 419672. Growth of two new peaks between 90 and 100 ppm is highlighted. Relaxation times and dextrose equivalent values are also shown

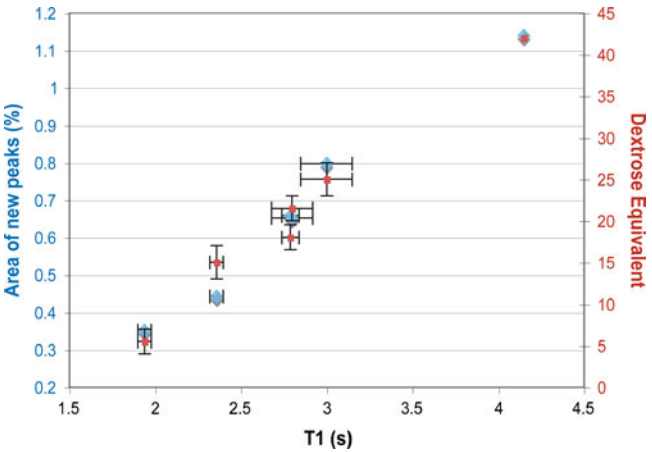

Fig. 8. Relationship between relaxation times, growth of new peaks in maltodextrin and corn syrup solid samples, and dextrose equivalent

Similarly, Spectrum lot #2 can be identified as λ-carrageenan, as its peak positions and relative intensities fall within the range for all "known" λ-forms that were analyzed. The chemical shift values and intensities for Spectrum lot #1 appear to match up very well with the values for "known" ι-forms, with one exception. As can be seen in Table III, the relative intensity of peak #6 for Spectrum lot #1 falls above the range for the "known" ι-forms. Considering this peak corresponds to the most intense signal (peak #5) in the κ-forms, it can be concluded that Spectrum lot #1 consists of primarily ι-form with some κ-form impurity. Thus, analysis of relative peak intensities provides insight into the purity of a carrageenan sample compared to known standards. However, the high degree of peak overlap makes it difficult to accurately detect and quantitate low levels of other forms that may be present as impurities.

Starch and Derivatives

Starch is one of the most abundant polymers in nature and contains two distinct polysaccharides, the linear amylose, and the highly branched amylopectin (17). The structure of starch consists of crystalline amylopectin clusters separated by disordered zones composed of amorphous material and/or amylose-lipid inclusion complexes (17–21). X-ray diffraction studies have shown that there are three types of crystalline polymorphs, referred to as A, B, and C (18). A- and B-type starch polymorphs are most common and consist of ordered arrays of double helices with similar conformations but different packing arrangements (17–19). The amylose-lipid inclusion complex is referred to as the V-type, which, unlike A- and B-type crystalline forms, consists solely of a single helix (17–21). Common sources of starch such as corn and wheat are

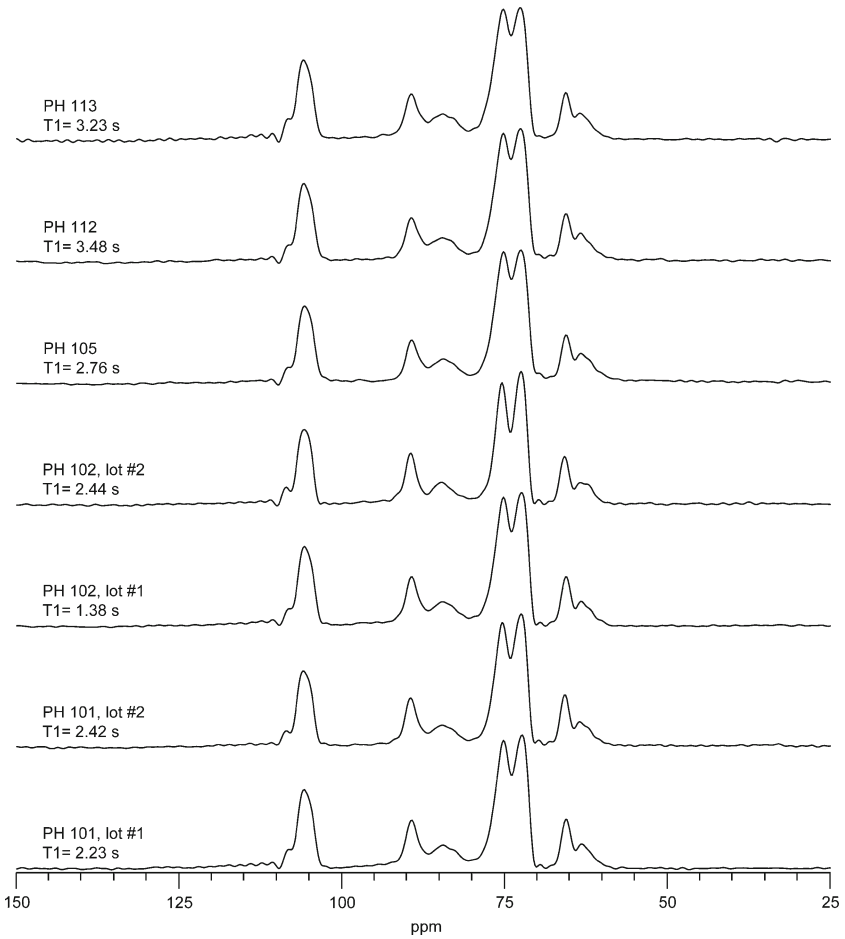

Fig. 9. ^{13}C SSNMR spectra and relaxation times of Avicel (FMC Biopolymer's trade name for microcrystalline cellulose) samples

classified as A-type, while starch from potato is classified as B-type.

The ^{13}C SSNMR spectra of the corn, wheat, and potato starch samples received from Sigma are shown in Fig. 5a, b, and c, respectively. Distinct differences in the C-1 region (90–110 ppm) are highlighted. It is well established that the C-1 resonance for A-type starches is split into three distinct SSNMR signals and for B-type starches into two distinct SSNMR signals (19–21). While a cluster of three peaks at approximately 101.5, 100.4, and 99.4 ppm is seen in both the corn and wheat A-type starches, there is also a broad peak present downfield at ~103 ppm in these samples. It has been reported that this peak is made up of signals from amorphous material and the V-type amylose-lipid complex (21,22). This peak is very large in the potato starch sample from Sigma (Fig. 5c). The large amount of amorphous or amylose content in this material could explain the difficulties in differentiating the two distinct peaks in the C-1 signal for this B-type starch.

An overlay of the ^{13}C SSNMR spectra of three cornstarch samples is shown in Fig. 6. The three C-1 signals typical of crystalline A-type starches are clearly observed in all samples. However, a fourth peak is also present in this region for all three samples. Deconvolution of this cluster of four peaks allows for integration of areas and calculation of the amount of crystalline A-type *versus* amorphous and V-type content present in each sample. SSNMR spectroscopy has recently been shown to be a superior method to PXRD for calculating starch crystallinity (23,24). The amount of crystalline content in the Sigma, Grain Processing B700, and Grain Processing B880 samples was calculated and found to be similar, with values of 61.1%, 59.6%, and 58.0%, respectively. However, it should be noted that there is likely some contribution from amorphous material to the area of the peaks assigned as crystalline, which could result in overestimation of crystalline content (24). In order to achieve more accurate values, a SSNMR spectrum of a purely amorphous starch standard would need to be obtained and then subtracted from the spectrum of the semicrystalline samples (24). Thus, while detection of small changes in percent crystallinity between starch samples may require more extensive analysis, significant differences can be easily detected by simply looking at the relative intensities of the three C-1 signals. Therefore, SSNMR spectroscopy can be used to identify the source (corn, wheat, potato) as well as to determine the amounts of amorphous and crystalline material present in the starch.

Maltodextrins and corn syrup solids are produced from either acid or enzymatic hydrolysis of starch (25). The degree of hydrolytic conversion of starch to these products is analytically referred to as the dextrose equivalent (DE), which is a measure of the total reducing power of the sugar relative to dextrose (25). Maltodextrins have DE values <20 while corn syrup solids are more extensively hydrolyzed products with DE values >20.

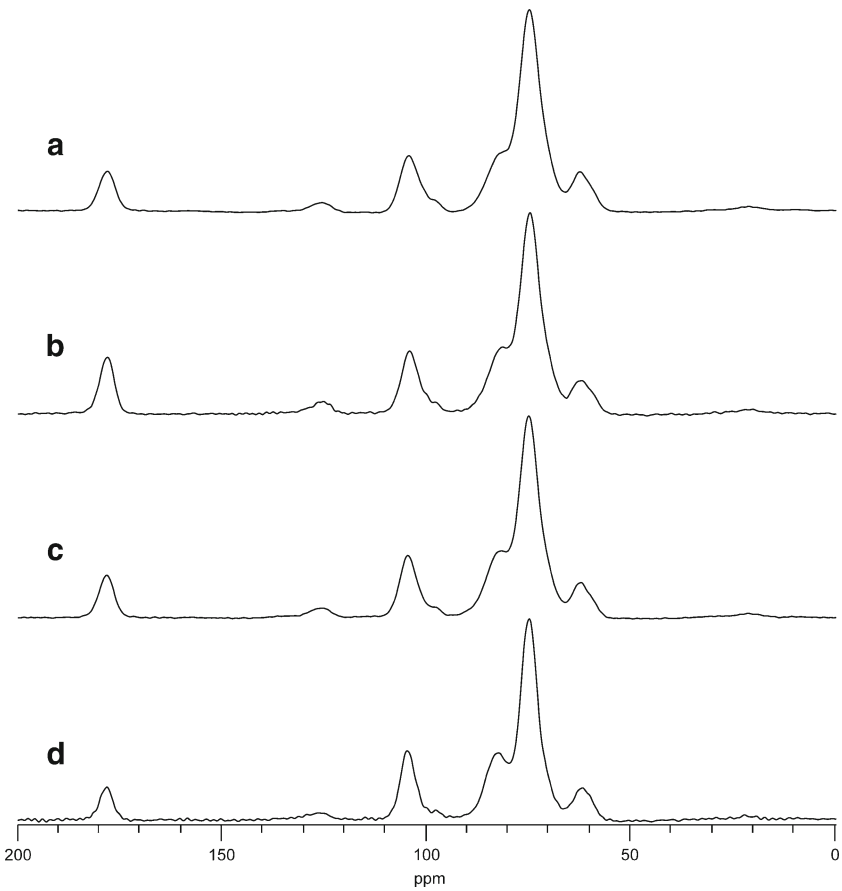

Fig. 10. ^{13}C SSNMR spectra of carboxymethylcellulose samples received from Acros Organics (**a**–**c**) and FMC Biopolymer (**d**)

^{13}C SSNMR spectra of several maltodextrin and corn syrup solids samples are shown in Fig. 7. Two peaks at ~93 and 97 ppm grow as the DE value (provided by the supplier) of the material increases. As the starch is hydrolyzed, species with lower molecular weights and shorter chains are being formed, which results in more end groups being produced. The carbons in these end groups are responsible for the new signals seen between 90 and 100 ppm in the SSNMR spectra. In addition, the ^{1}H T_1 values range from as low as 1.94 s to as high as 4.15 s and appear to increase as the DE value of the material increases (Fig. 7). These values are higher than the ^{1}H T_1 values for the starch samples, which were between 0.8 and 0.9 s. This suggests a relationship between degree of hydrolysis and SSNMR proton relaxation time seems to exist. To better examine this relationship, a plot of the peak area of the signals between 90 and 100 ppm *versus* ^{1}H T_1 value was made and is shown in Fig. 8. The areas of the peaks at ~93 and 97 ppm were normalized to the area of the peak denoted as 1 in Fig. 7 and then the normalized area percentage of these peaks was calculated. As illustrated in Fig. 8, a direct correlation between the area of these peaks and the relaxation time of the sample is observed. The DE value range provided by the supplier is also plotted for comparison. The overlap between the blue data points (peak area) and red data points (DE value range) is strong, showing that the relaxation values and peak areas of starch derivatives such as maltodextrin and corn syrup solids can be related to the degree of hydrolysis. Interestingly, this suggests that SSNMR data can be used to determine differences in the degree of hydrolysis between starch derivatives, potentially providing an attractive alternative method for determining differences in DE values among various samples.

Microcrystalline Cellulose and Cellulose Derivatives

Microcrystalline cellulose is one of the most commonly used pharmaceutical excipients for direct tableting. Differences in flow properties and tableting characteristics can be attributed to differences in moisture content and particle size distribution (26), and microcrystalline cellulose is typically available as grades that are classified according to these parameters. Multiple grades of microcrystalline cellulose varying in mean particle size and water content were received from FMC Biopolymers, as shown in Table I. The SSNMR spectra and corresponding ^{1}H T_1 values of all of the samples analyzed are shown in Fig. 9. There are no significant differences observed between the spectra of different grades or between lots of the same grade. However, there are noticeable differences in relaxation times. The ^{1}H T_1 values of grades PH-112 and PH-113 appear to be higher than those of PH-101, PH-102, and PH-105. This can be explained by differences in water

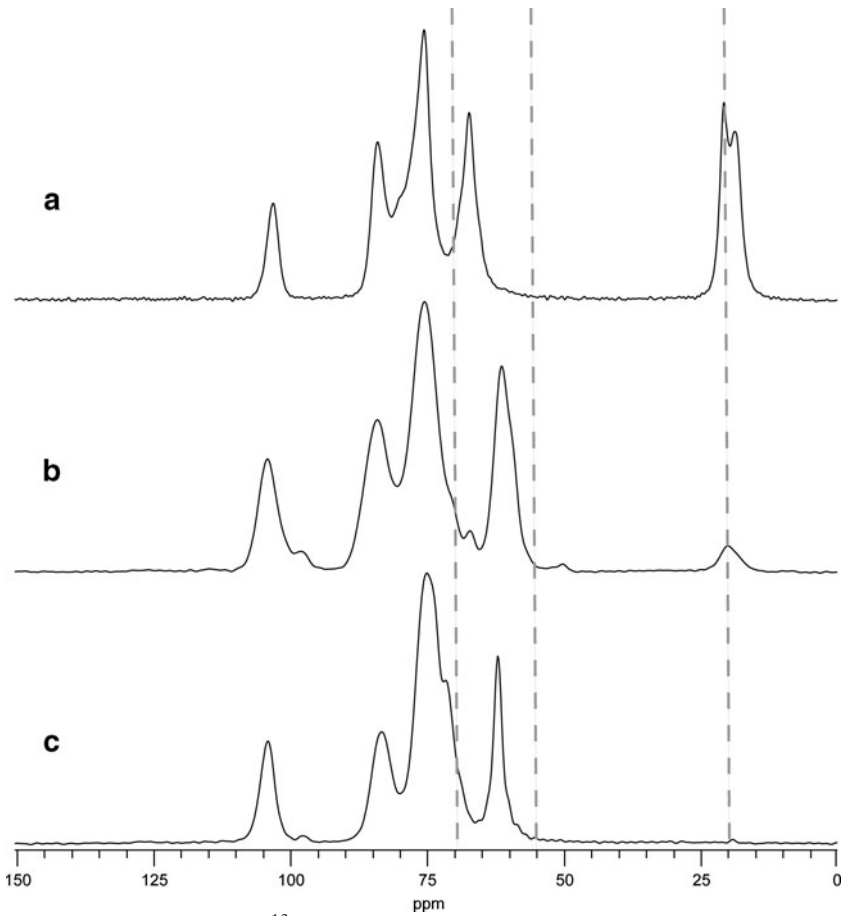

Fig. 11. Representative ^{13}C SSNMR spectra of **a** hydroxypropylcellulose, **b** hydroxypropylmethylcellulose, and **c** hydroxyethylcellulose. Key differences in the spectra are highlighted

content. According to the specifications provided by the manufacturer, grades PH-112 and PH-113 contain lower amounts of water than the others. This was confirmed using TGA. The PH-112 and PH-113 grades had water contents between 2.0% and 2.5%, while the PH-101, PH-102, and PH-105 grades all had water contents between 3.5% and 4.0%. Thus, the higher relaxation times of the PH-112 and PH-113 grades are likely caused by the reduced mobility of these samples compared to the others in which more water is present. Additionally, lot-to-lot variations in the ^{1}H T_1 values for grade PH-102 were observed (Fig. 9). The first lot of PH-102 had a relaxation time much lower than that of the second lot of this grade. TGA was performed on these samples in order to detect differences in water content that could potentially explain the observed differences in relaxation times between lots. The first lot of PH-102 had a water content of 4.1% by TGA, while the water content of the second lot was measured as 3.8%. This slight difference in water content does not explain the significant decrease in ^{1}H T_1 for the first lot. Other factors such as impurities or molecular weight differences could possibly explain the difference, but the samples would have to be examined through further experimentation in order to confirm or deny these possible explanations.

The second cellulose-based excipient that was examined was carboxymethylcellulose sodium. This excipient is primarily used for its viscosity-increasing properties and is therefore available in a wide range of molecular weights (5). Three samples from Acros Organics differing in molecular weight were analyzed, along with one medium-viscosity grade sample from Fluka. The SSNMR spectra of these four samples are shown in Fig. 10. All three spectra of samples from Acros (Fig. 10a–c) look practically identical, while the spectrum of the sample from Fluka (Fig. 10d) appears slightly different, displaying better resolution of peaks in the 50–90 ppm region. All of the samples had ^{1}H T_1 values of ~2 s, except for one Acros sample that had a ^{1}H T_1 value of 4.6 s. This difference in relaxation time did not appear to correlate with molecular weight and viscosity. However, results from TGA analysis showed that all samples except for the one Acros lot exhibiting a longer relaxation time had water contents between 9.5% and 10%. The Acros sample with a ^{1}H T_1 value of 4.6 s had a water content of only 6.1%. Therefore, the reduced mobility of this sample might be attributed to a much lower water content compared to the others.

Cellulose derivatives such as HEC, HPC, and HPMC were also analyzed. These excipients are partially substituted derivatives of cellulose and are available as several grades

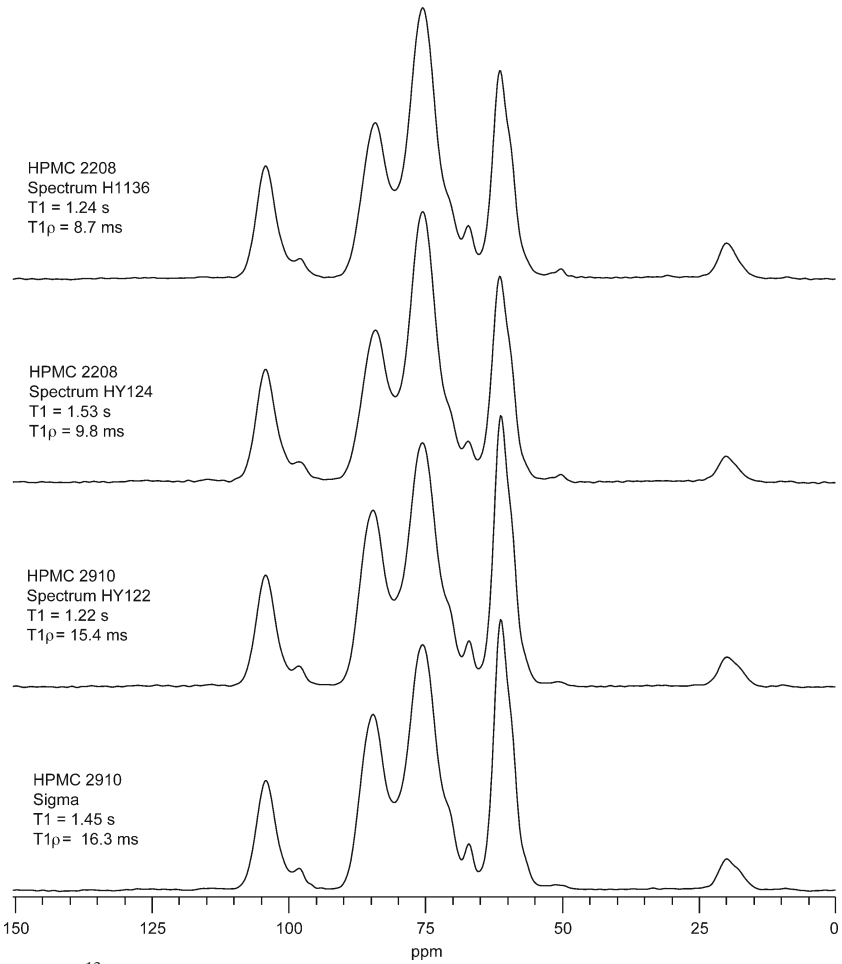

Fig. 12. ^{13}C SSNMR spectra of type 2208 and type 2910 hydroxypropylmethylcellulose samples. Differences in peak intensity at ~60 ppm are due to differences in methoxy content. ^{1}H $T_{1\rho}$ values differ for these two types

that vary in viscosity and the extent of substitution (5). HPMC grades are also further designated according to the relative percentage of methoxy and hydroxypropoxy groups present. These parameters are key properties known to be important to the performance of these excipients in pharmaceutical formulations (27). Representative SSNMR spectra for each of these substituted cellulose derivatives are shown in Fig. 11. Differences between the spectra are highlighted and are due to the varying number and types of CH, CH_2, and CH_3 groups present in each sample. Specifically, the peak below 25 ppm corresponds to a methyl group that is not directly attached to an oxygen atom. HPC contains the greatest amount of these types of methyl groups, followed by HPMC. The HEC samples do not contain these groups; therefore, the SSNMR spectra of these samples do not contain any peaks below 50 ppm. Distinct differences between HEC, HPC, and HPMC in the 55–70 ppm region of the SSNMR spectra are also observed. There were no noticeable differences between spectra and relaxation times for all of the HEC and HPC samples that were studied. However, HPMC type 2208 and 2910, which differ in the number of methoxy and hydroxypropoxy groups, showed distinct differences in their SSNMR spectral details. As shown in Fig. 12, the peak located at ~60 ppm is more intense in type 2910 samples than in the 2208 samples. This is due to the greater methoxy content present in the 2910 samples. Type 2910 HPMC contains 28–30% methoxy, while type 2208 contains 19–24%. The observed differences in the SSNMR spectra allow these two types of HPMC to be clearly distinguished from each other. Another very interesting observation is the difference in ^1H $T_{1\rho}$ values between the two types of HPMC (Fig. 12). Although all samples had similar ^1H T_1 values (1.2–1.5 s), the type 2910 samples showed a ^1H $T_{1\rho}$ value equal to almost double that of the 2208 samples. The greater methoxy content restricts the mobility of type 2910 samples in comparison to 2208 samples, which have a greater amount of hydroxypropoxy groups, longer chains, and hence more flexibility. Thus, ^1H $T_{1\rho}$ is another SSNMR parameter that can potentially be used to distinguish between these two types of HPMC.

CONCLUSIONS

Important characteristics of naturally derived excipients such as form identification, structural differences, crystalline and amorphous content, and water content variations can be detected using SSNMR spectroscopy experiments. SSNMR spectroscopy offers the unique advantages of (1) non-destructive sample preparation and (2) selectivity. Therefore, SSNMR spectroscopy can potentially be used to monitor changes in excipients present in solid dosage forms without any alteration to the sample. This could be very useful during preformulation and formulation stages, particularly when the source of an excipient changes, or when manufacturing and/or storage conditions could potentially alter the excipient.

ACKNOWLEDGEMENTS

The authors thank the USP for their assistance in gathering the samples for analysis. The authors acknowledge Lucas McCormick for his contribution to this project during an undergraduate summer internship at the University of Kansas. EJM and DMS acknowledge funding from NSF grant CHE0719464. DMS also acknowledges funding from the Takeru Higuchi Predoctoral Fellowship and the Madison and Lila Self Graduate Fellowship at the University of Kansas.

REFERENCES

1. Moreton C. Functionality and performance of excipients in quality-by-design world part 4: obtaining information on excipient variability for formulation design space. Am Pharm Rev. 2009;12:28–32.
2. Vogt F. A multi-disclipinary approach to the solid-state analysis of pharmaceuticals. Am Pharm Rev. 2008;11:50–7.
3. Berendt R, Sperger D, Isbester P, Munson E. Solid-state NMR spectroscopy in pharmaceutical research and analysis. Trends Anal Chem. 2006;25:977–84.
4. Lubach J, Dawie X, Segmuller B, Munson E. Investigation of the effects of pharmaceutical processing upon solid-state NMR relaxation times and implications to solid-state formulation stability. J Pharm Sci. 2007;96:777–87.
5. Rowe R, Sheskey P, Owen S. Handbook of pharmaceutical excipients. 5th ed. Washington, DC: Pharmaceutical Press and the American Pharmacists Association; 2006.
6. Pines A, Gibby M, Waugh J. Proton-enhanced NMR of dilute spins in solids. J Chem Phys. 1973;59:569–90.
7. Andrew E. Narrowing of NMR spectra of solids by high-speed specimen rotation and the resolution of chemical shift and spin multiplet structures for solids. Prog Nucl Magn Reson. 1971;8:1–39.
8. Dixon W, Schaefer J, Sefcik M, Stejskal E, McKay R. Total suppression of sidebands in CPMAS carbon-13 NMR. J Magn Reson. 1982;49:341–5.
9. Fung B, Khitrin A, Ermolaev K. An improved broadband decoupling sequence for liquid crystals and solids. J Magn Reson. 2000;142:97–101.
10. Barich D, Gorman E, Zell M, Munson E. 3-methylglutaric acid as a ^{13}C solid-state NMR standard. Nucl Magn Reson. 2006;30:125–9.
11. Haug A, Larsen B, Smidsrod O. A study of the constitution of alginic acid by partial acid hydrolysis. Acta Chem Scand. 1966;20:183–90.
12. Grasdalen H, Larsen B, Smidsrod O. A P.M.R. study of the composition and sequence of uronate residues in alginate. Carbohydr Res. 1979;68:23–31.
13. Llanes F, Sauriol F, Morin G, Perlin A. An examination of sodium alginate from sargassum by NMR spectroscopy. Can J Chem. 1997;75:585–90.
14. Salomonsen T, Jensen H, Larsen F, Steuernagel S, Engelsen S. Direct quantification of M/G ratio from ^{13}C CP-MAS NMR spectra of alginate powders by multivariate curve resolution. Carbohydr Res. 2009;344:2014–22.
15. Anderson N, Dolan T, Rees D. Evidence for a common structural pattern in the polysaccharide sulphates of the rhodophyceae. Nature. 1965;205:1060–2.
16. Rochas C, Lahaye M. Solid state 13 C-NMR spectroscopy of red seaweeds, agars and carrageenans. Carbohydr Polym. 1989;10:189–204.
17. Imberty A, Buleon A, Tran V, Perez S. Recent advances in knowledge of starch structure. Starch. 1991;43:375–84.
18. Sarko A, Wu H. The crystal structures of A-B- and C-polymorphs of amylose and starch. Starch. 2006;30:73–8.
19. Gidley M, Block S. Molecular organizations in starches: a ^{13}C CP/MAS NMR study. J Am Chem Soc. 1985;107:7040–4.
20. Veregin R, Fyfe C. Characterization of the crystalline A and B starch polymorphs and investigation of starch crystallization by high-resolution ^{13}C CP/MAS. Macromolecules. 1986;19:1030–4.
21. Morgan K, Furneaux R, Larsen N. Solid-state NMR studies on the structure of starch granules. Carbohydr Res. 1995;276:387–99.

22. Gidley M, Bociek S. ^{13}C CP/MAS NMR studies of amylose inclusion complexes, cyclodextrins, and the amorphous phase of starch granules: relationships between glycosidic linkage conformation and solid-state ^{13}C chemical shift. J Am Chem Soc. 1988;110:3820–9.
23. Lopez-Rubio A, Flanagan B, Gilbert E, Gidley M. A novel approach for calculating starch crystallinity and its correlation with double helix content: a combined PXRD and NMR study. Biopolymers. 2008;89:761–8.
24. Tan I, Flanagan B, Halley P, Whittaker A, Gidley M. A method for estimating the nature and relative proportions of amorphous, single, and double-helical components in starch granules by ^{13}C CP/MAS NMR. Biomacromolecules. 2007;8:885–91.
25. Dokic L, Jakovljevic J, Dokic P. Relation between viscous characteristics and dextrose equivalent of maltodextrins. Starch. 2004;56:520–5.
26. Doelker E, Mordier D, Iten H, Humbert-Droz P. Comparative tableting properties of sixteen microcrystalline celluloses. Drug Dev Ind Pharm. 1987;13:1847–75.
27. Mitchell S, Balwinski K. A framework to investigate drug release variability arising from hypromellose viscosity specifications in controlled release matrix tablets. J Pharm Sci. 2008;97:2277–85.